(Received 25 January 2024, Accepted 9 March 2024, Scheduled 19 March 2024)

A Wide Adaptation Variable Step-Size Adaline Neural Network Parameter Identification IPMSM Model Predictive Control Strategy

Qianghui Xiao[1], Xingwang Chen[1], Zhun Cheng[2,*], Zhongjian Tang[1], and Zhi Yu[1]

[1] *Hunan University of Technology, Zhuzhou 412007, China*
[2] *Hunan Railway Professional Technology College, Zhuzhou 412001, China*

ABSTRACT: Model predictive control (MPC), as a frequently adopted control strategy for permanent magnet synchronous motors (PMSMs), exhibits favorable dynamic response capabilities. However, it necessitates an accurate mathematical model of the controlled object, and any parameter mismatch can lead to a decline in control performance. This paper proposes a model predictive current control (MPCC) method based on parameter identification, which can be extended to the parameter identification of plug-in permanent magnet synchronous motors (IPMSMs). A wide-adaptability variable step-size algorithm is designed in response to the varying effects of single variable step-size functions on parameter convergence speed and ripple when the motor experiences different parameter disturbances. This method classifies and fits various variable step-size functions based on the maximum value of the absolute value of different instantaneous errors. This allows different variable step-size functions to adapt to different parameter disturbances, resulting in rapid waveform convergence and consistent ripple size in the identification process. Additionally, a new variable step-size function type was designed with simple parameter settings and easy debugging. Finally, the effectiveness of the proposed method was verified through experiments, and the results showed that the method can achieve fast and accurate identification of multiple parameters under different parameter perturbations, ensuring stable current control.

1. INTRODUCTION

PMSMs are widely used in industrial automation, electric vehicles, aerospace, and other fields due to their high power density, high efficiency, precise control, and long life. PMSM system is a complex control system with nonlinear and strong coupling characteristics, making it challenging to achieve satisfactory control performance with linear current control methods such as PI. Currently, there are some relatively mature control strategies, such as sliding mode control, fuzzy control, and MPC [1–6].

MPC has good dynamic response performance and can quickly track command signals without overshoot, but the current prediction process is affected by various factors, such as motor parameter mismatch, digital control system delay, and inverter nonlinearity [7–10]. In order to optimize the MPC control algorithm and reduce the current prediction error, that is, the difference between the predicted value and the actual measured value, it is necessary to consider better operating conditions and perform necessary error compensation. In response to the problem of prediction error, many experts and scholars have proposed solutions and improvements, such as designing disturbance observer methods, direct compensation methods for prediction errors, model-free predictive current control, and parameter identification methods [11–14]. Among them, the parameter identification method can fundamentally reduce the impact of parameter mismatch on the system by identifying the stator resistance, dq-axis inductance, and permanent magnet flux linkage of the permanent magnet synchronous motor.

According to whether the PMSM is in online operation, parameter identification methods can be divided into offline identification and online identification. Offline identification cannot track the changes in motor parameters in real time and can only obtain the identification results of motor parameters through steady-state calculations based on collected information such as motor voltage, current, and speed. In order to obtain the parameters of the motor in real time, online identification strategy can be adopted. Common PMSM identification algorithms include least squares method, extended Kalman filter algorithm, model reference adaptive system (MRAS) algorithm, and neural network algorithm. Ref. [15] uses the method of fixing the magnetic flux parameters in the MRAS adjustable model to identify the resistance and inductance parameters. However, if there is a deviation between the magnetic flux values in the model and actual magnetic flux values, it will lead to identification errors in the resistance and inductance. To overcome the problem of low rank, [16] obtains the high-frequency characteristics of the motor by injecting high-frequency voltage to increase the state equation, thereby achieving multi-parameter identification. Ref. [17] uses cur-

* Corresponding author: Zhun Cheng (120277982@qq.com).

rent injection to construct a new motor state equation during steady-state operation of the motor, solving the problem of low rank in multi-parameter identification. However, the current injection method may have an impact on the operating state of the motor. Ref. [18] proposes the concept of quasi-steady state, which achieves simultaneous multi-parameter identification of the motor by constructing a steady-state equation for the motor under different speed conditions. However, the identification process requires continuous adjustment of the operating state of the motor, and the control process is complex. In recent years, neural network algorithms have been used for parameter identification of PMSM and have achieved good results. Ref. [19] introduces a single-layer neural network with gradient descent into motor parameter identification. Although the identification speed converges quickly, the reliability of the identification results is low. Ref. [20] proposes a parameter identification method based on adaptive linear element neural network. This method utilizes d-axis current injection to construct a new state equation for the motor when it is stationary. It not only solves the rank-deficient problem in multi-parameter identification of motors, but also considers the impact of nonlinear factors corresponding to the inverter on the system. Although this method has low computational complexity and high identification accuracy, the multi-parameter identification process cannot be performed simultaneously. A variable step size Adaline neural network parameter identification method is proposed in [21]. This method constrains the step size by establishing a functional relationship between instantaneous error and step size, effectively reducing the steady-state error of motor parameter identification while improving the convergence rate of the identification results. However, when the instantaneous error is very small, there is a problem of too fast step-size change, which will affect the stability of the identification process. In response to this problem, [22] proposes a new variable step-size function that improves the stability of the identification process when the instantaneous error is very small. Moreover, this function introduces a speed factor to ensure the performance of the identification algorithm at different speeds. However, when there are varying degrees of parameter mismatch in the motor, this algorithm cannot guarantee consistency between identification speed and identification accuracy.

To address the above issues, this paper replaces the simplified motor mathematical model based on traditional neural network parameter identification algorithm with a current prediction error model, making the proposed algorithm applicable to parameter identification of IPMSM. In addition, based on the relationship between motor parameter mismatch and the maximum absolute value of instantaneous error, this paper maps different larger values of instantaneous error to different variable step functions. This enables the motor to correspond to different variable step functions under different degrees of parameter mismatch, ensuring consistency in the recognition speed and recognition accuracy of the algorithm. Finally, this paper proposes a new variable step-size function, which is simpler to tune and easier to debug than traditional variable step-size functions.

2. MPCC THEORY AND CURRENT PREDICTION ERROR MODEL

2.1. MPCC Theory

The stator current equation of the permanent magnet synchronous motor in the synchronous rotating coordinate system (d-q) is as follows:

$$\begin{cases} L_d \frac{di_d}{dt} = -Ri_d + \omega L_q i_q + u_d \\ L_q \frac{di_q}{dt} = -Ri_q - \omega L_d i_d + u_q - \omega\psi_f \end{cases} \tag{1}$$

where L_d is the stator d-axis inductance; L_q is the stator q-axis inductance; R is the stator resistance; ω is the rotor electrical angular velocity; ψ_f is the rotor permanent magnet flux linkage; i_d is the stator current d-axis current component; i_q is the stator current q-axis current component; u_d is the stator voltage d-axis voltage component; u_q is the stator voltage q-axis voltage component.

The discrete dq-axis current prediction equation for the next sampling moment can be approximated by the Euler discretization method:

$$\begin{cases} i_d(k+1) = \left(1 - \frac{T_s R}{L_d}\right) i_d(k) + \frac{T_s L_q}{L_d} \omega(k) i_q(k) \\ \qquad\qquad + \frac{T_s}{L_d} u_d(k) \\ i_q(k+1) = \left(1 - \frac{T_s R}{L_q}\right) i_q(k) - \frac{T_s L_d}{L_q} \omega(k) i_d(k) \\ \qquad\qquad + \frac{T_s}{L_q} u_q(k) - \frac{T_s \psi_f}{L_q} \omega(k) \end{cases} \tag{2}$$

where T_s is the control period.

Use (2) to calculate the predicted values of the d-axis and q-axis currents corresponding to the eight basic voltage vectors, and then substitute them into the value function (3). The voltage vector that minimizes the value function is selected as the optimal voltage vector and is output by the inverter.

$$g_i = \left[i_d^* - i_d(k+1)\right]^2 + \left[i_q^* - i_q(k+1)\right]^2 \tag{3}$$

where i_d^* and i_q^* are the d-axis and q-axis current commands, respectively.

2.2. Current Prediction Error Model

According to the prediction model (2), when there is a parameter mismatch in the motor, the current prediction model can be expressed as follows:

$$\begin{cases} i'_d(k+1) = \left[1 - \frac{T_s(R+\Delta R)}{L_d+\Delta L_d}\right] i_d(k) \\ \qquad + \frac{T_s(L_q+\Delta L_q)}{L_d+\Delta L_d} \omega(k) i_q(k) + \frac{T_s}{L_d+\Delta L_d} u_d(k) \\ i'_q(k+1) = \left[1 - \frac{T_s(R+\Delta R)}{L_q+\Delta L_q}\right] i_q(k) \\ \qquad - \frac{T_s(L_d+\Delta L_d)}{L_q+\Delta L_q} \omega(k) i_d(k) + \frac{T_s}{L_q+\Delta L_q} u_q(k) \\ \qquad - \frac{T_s(\psi_f+\Delta\psi_f)}{L_q+\Delta L_q} \omega(k) \end{cases} \tag{4}$$

where ΔR, ΔL_d, ΔL_q, and $\Delta\psi_f$ are the differences between the actual values and reference values of resistance, d-axis inductance, q-axis inductance, and permanent magnet flux linkage, respectively. Subtracting (4) from (2) yields the current

prediction error model as follows:

$$\begin{cases} E_d = i'_d(k+1) - i_d(k+1) \\ \quad = \frac{T_s R\Delta L_d - T_s \Delta R L_d}{L_d(L_d+\Delta L_d)} i_d(k) - \frac{T_s \Delta L_d}{L_d(L_d+\Delta L_d)} u_d(k) \\ \quad + \frac{T_s \Delta L_q L_d - T_s L_q \Delta L_d}{L_d(L_d+\Delta L_d)} \omega(k) i_q(k) \\ E_q = i'_q(k+1) - i_q(k+1) \\ \quad = \frac{T_s R\Delta L_q - T_s \Delta R L_q}{L_q(L_q+\Delta L_q)} i_q(k) - \frac{T_s \Delta L_q}{L_q(L_q+\Delta L_q)} u_q(k) \\ \quad + \frac{T_s \Delta L_q L_d - T_s L_q \Delta L_d}{L_q(L_q+\Delta L_q)} \omega(k) i_d(k) \\ \quad + \frac{T_s \Delta L_q \psi_f - T_s L_q \Delta \psi_f}{L_q(L_q+\Delta L_q)} \omega(k) \end{cases} \tag{5}$$

From (5), it can be seen that any change in one parameter can cause current prediction errors. The relationship between current prediction errors and parameter mismatches is reflected in [23], from which it can be seen that parameter mismatches in inductance and permanent magnet flux linkage are the main factors that cause current prediction errors, while the impact of resistance mismatches is quite small and can be almost ignored.

Based on the above conclusion, the simplified model is obtained by substituting $\Delta R = 0$ into (5):

$$\begin{cases} E_d = A_d \frac{T_s[Ri_d(k) - u_d(k)]}{L_d} + A_q \frac{T_s L_q \omega(k) i_q(k)}{L_d} \\ E_q = B_q \frac{T_s[Ri_q(k) - u_q(k)]}{L_q} + B_d \frac{T_s L_d \omega(k) i_d(k)}{L_q} \\ \quad + C_{\psi_f} \frac{T_s \omega(k) \psi_f}{L_q} \end{cases} \tag{6}$$

$$\begin{cases} A_d = \frac{\Delta L_d}{L_d + \Delta L_d} \\ A_q = \frac{\Delta L_q L_d - L_q \Delta L_d}{L_q(L_d + \Delta L_d)} \\ B_q = \frac{\Delta L_q}{L_q + \Delta L_q} \\ B_d = \frac{\Delta L_q L_d - L_q \Delta L_d}{L_d(L_q + \Delta L_q)} \\ C_{\psi_f} = \frac{\Delta L_q \psi_f - L_q \Delta \psi_f}{\psi_f(L_q + \Delta L_q)} \end{cases} \tag{7}$$

3. TRADITIONAL ADALINE NEURAL NETWORK THEORY AND PARAMETER IDENTIFICATION ALGORITHM DESIGN

3.1. Adaline Neural Network Theory

The Adaline neural network is a linear neural network that can output any value. The function of the Adaline neural network is to compare its expected output with the actual simulated output, obtain an error signal that is also a simulated quantity, and continuously adjust the weight vector online based on the error signal to ensure that the expected output and actual simulated output remain equal at all times, thereby converting a set of input simulated signals into any desired waveform. Currently, this algorithm can be used for some dynamic systems with complex coupling relationships to identify system parameters. The basic structure of the Adaline neural network is shown in Figure 1.

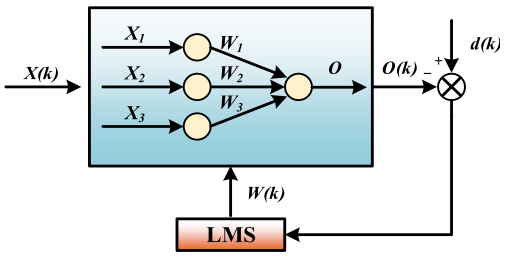

FIGURE 1. Basic structure of Adaline neural network.

The input and output relationship of the neural network is as follows:

$$O(W_i, X_i) = WX = \sum W_i X_i \tag{8}$$

The convergence expression of its weight value is as follows:

$$\begin{cases} W(k+1) = W(k) + 2\eta X(k)\varepsilon(k) \\ \varepsilon(k) = d(k) - O(k) \end{cases} \tag{9}$$

In (9), $W(k)$, $X(k)$, $O(k)$, and $d(k)$ represent the weight value, input, output, and target output of the network at time kT_s. In this algorithm, the actual value of each step-size is replaced by an estimated value of the gradient, eliminating the need for complex matrix solving. The iterative calculation requires only a small number of simple operations. Compared to model reference adaptive algorithms and extended Kalman filter algorithms, Adaline algorithm has significantly lower computational cost while ensuring convergence speed.

In order to ensure the convergence of the algorithm, the step-size η needs to satisfy the following conditions:

$$0 < 2\eta |X(k)|^2 < 1 \tag{10}$$

3.2. Design of Parameters Identifier for Traditional Adaline Neural Network Algorithm

In the permanent magnet synchronous motor control system, the control method of $I_d = 0$ is usually adopted. When the motor is operating steadily, the differential terms of the d-axis and q-axis in (1) and the d-axis current can be approximately equal to 0, so the steady-state voltage equation can be expressed as:

$$\begin{cases} u_d = -L_q \omega i_q \\ u_q = R i_q + \omega \psi_f \end{cases} \tag{11}$$

From (11), it can be seen that L_q is not coupled with other parameters and can be identified independently, while R and ψ_f are coupled and cannot be identified directly. Usually, the method of injecting current into the d-axis is used to increase the number of motor state equations and achieve online parameter identification. Additionally, use (11) to add the motor state equation by subtracting the values at two different time points, and then identify R based on the added motor state equation. These two methods cannot identify both R and ψ_f at the same time, requiring the identification of R before the identification of ψ_f, which greatly affects the identification speed of ψ_f. Considering that the change in resistance has a small impact on current prediction error, this article will not identify resistance. The average value of both sides of the two equations in (11) can reduce the influence of nonlinear factors in the inverter on

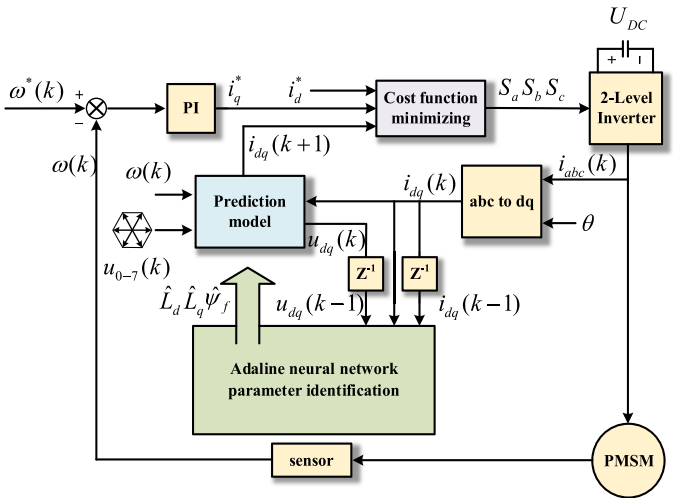

FIGURE 2. Basic structure diagram of MPCC based on Adaline neural network parameter identification.

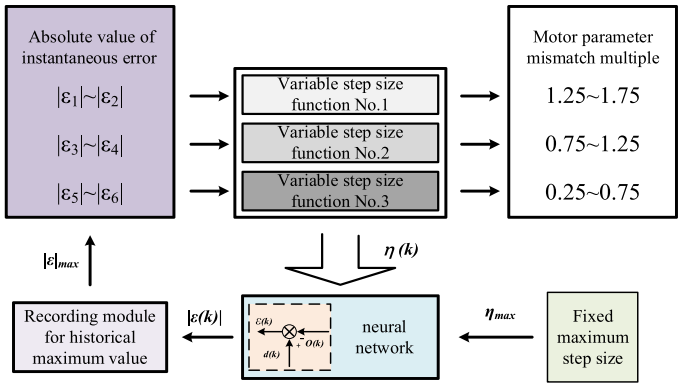

FIGURE 3. Block diagram of the structure of the wide adaptation variable step-size strategy.

parameter identification. Therefore, the final identification algorithm design is as follows:

1) q-axis inductance identifier

According to the first equation in formula (11), the identification algorithm for q-axis inductance is designed as follows:

$$\begin{cases} X_{L_q}(k) = -\bar{\omega}(k)\bar{i}_q(k) \\ O_{L_q}(k) = L_q(k)X_{L_q}(k) \\ d_{L_q}(k) = \bar{u}_d(k) \\ L_q(k+1) = L_q(k) + 2\eta(k)X_{L_q}(k)\varepsilon(k) \end{cases} \tag{12}$$

2) Rotor permanent magnet flux identifier

According to the second equation in formula (11), the identification algorithm for the rotor permanent magnet flux linkage is designed as follows:

$$\begin{cases} X_{\psi_f}(k) = \bar{\omega}(k) \\ O_{\psi_f}(k) = \psi_f(k)X_{\psi_f}(k) \\ d_{\psi_f}(k) = \bar{u}_q(k) - R\bar{i}_q \\ \psi_f(k+1) = \psi_f(k) + 2\eta(k)X_{\psi_f}(k)\varepsilon(k) \end{cases} \tag{13}$$

The above Adaline neural network algorithm proposes a strategy of taking the average of the input and target output of the identification algorithm. Although this improves the stability of the identification, the resulting convergence speed of the identification is also slowed down, and there is a certain lag in the identification process, which makes the identification time longer. For applications that require simultaneous identification of d-axis inductance and q-axis inductance, due to the limitations of its mathematical model, the traditional Adaline neural network algorithm can only identify the q-axis inductance. Based on the above problems, this paper proposes an Adaline neural network parameter identification algorithm based on current prediction error model. This algorithm does not require taking the average of any part, and compared to the above traditional algorithm, it has faster identification speed, higher identification accuracy, and is more suitable for multi-parameter identification.

3.3. Design of Adaline Neural Network Algorithm Parameter Identifier Based on Current Prediction Error Model

From the above analysis, it can be seen that the traditional Adaline neural network algorithm parameter identification model based on the model is not applicable to the environment of IPMSM parameter identification. To solve this problem, without considering the influence of resistance changes, the current prediction error model (6) can be used as a new Adaline neural network parameter identification model. This model contains the disturbance information of parameters L_d, L_q, and ψ_f, and can indirectly identify parameters L_d, L_q, and ψ_f by identifying weights A_d, A_q, B_d, B_q, and C_{ψ_f}. To make the identification process more concise and understandable, (7) is simplified to:

$$\begin{cases} A_d = \frac{\alpha}{1+\alpha} \\ A_q = \frac{\beta-\alpha}{1+\alpha} \\ B_q = \frac{\beta}{1+\beta} \\ B_d = \frac{\beta-\alpha}{1+\beta} \\ C_{\psi_f} = \frac{\beta-\gamma}{1+\beta} \end{cases} \tag{14}$$

In (14), α, β, and γ represent the change multipliers of parameters L_d, L_q, and ψ_f, respectively.

In (6), the second term of the two equations is usually much smaller than the other terms, which means that small perturbations in the other terms can cause large fluctuations in the identification of the weight value in the second term, making it impossible for the weight value to stabilize at the target value and making it impossible to accurately identify the parameter represented by this term. To address this issue, under the premise of ensuring smaller identification errors, Adaline neural network IPMSM parameter identification algorithm is designed by taking A_d, B_q, and C_{ψ_f} as the identification conditions for α, β, and γ, and finally obtaining the current parameters L_d, L_q, and

ψ_f represented by α, β, and γ, respectively. Based on the above analysis, the Adaline neural network IPMSM parameter identification algorithm based on current prediction error model is designed as follows:

1) d-axis inductance identifier

According to (6), (7), and (14), the identification algorithm for the d-axis inductance is designed as follows:

$$\begin{cases} X_{A1}(k) = \frac{T_s[Ri_d(k)-u_d(k)]}{L_d} \\ X_{A2}(k) = \frac{T_s L_q \omega(k) i_q(k)}{L_d} \\ O_{L_d}(k) = A_d(k)X_{A1}(k) + A_q(k)X_{A2}(k) \\ d_{L_d}(k) = i_d^m(k+1) - i_d^P(k+1) \\ A_d(k+1) = A_d(k) + 2\eta(k)X_{A1}(k)\varepsilon_{L_d}(k) \\ A_q(k+1) = A_q(k) + 2\eta(k)X_{A2}(k)\varepsilon_{L_d}(k) \\ \alpha(k+1) = \frac{A_d(k+1)}{1-A_d(k+1)} \\ L_d(k+1) = [1+\alpha(k+1)]L_d \end{cases} \tag{15}$$

In (15), $i_d^m(k+1)$ and $i_d^p(k+1)$ represent the measured and predicted values of the d-axis current at time $(k+1)T_s$, respectively.

2) d-axis identifier and rotor permanent magnet flux linkage identifier

According to (6), (7), and (14), the identification algorithm for the q-axis inductance and rotor permanent magnet flux linkage is designed as follows:

$$\begin{cases} X_{B1}(k) = \frac{T_s[Ri_q(k)-u_q(k)]}{L_q} \\ X_{B2}(k) = \frac{T_s L_d \omega(k) i_d(k)}{L_q} \\ X_{C1}(k) = \frac{T_s \omega(k) \psi_f}{L_q} \\ O_{L_q+\psi_f}(k) = B_q(k)X_{B1}(k) + B_d(k)X_{B2}(k) \\ \qquad\qquad +C_{\psi_f}X_{C1}(k) \\ d_{L_q+\psi_f}(k) = i_q^m(k+1) - i_q^P(k+1) \\ B_q(k+1) = B_q(k) + 2\eta(k)X_{B1}(k)\varepsilon_{L_q+\psi_f}(k) \\ B_d(k+1) = B_d(k) + 2\eta(k)X_{B2}(k)\varepsilon_{L_q+\psi_f}(k) \\ C_{\psi_f}(k+1) = C_{\psi_f}(k) + 2\eta(k)X_{C1}(k)\varepsilon_{L_q+\psi_f}(k) \end{cases} \tag{16}$$

$$\begin{cases} \beta(k+1) = \frac{B_q(k+1)}{1-B_q(k+1)} \\ \gamma(k+1) = [1-C_{\psi_f}(k+1)]\beta(k+1) \\ \qquad\qquad -C_{\psi_f}(k+1) \\ L_q(k+1) = [1+\beta(k+1)]L_q \\ \psi_f(k+1) = [1+\gamma(k+1)]\psi \end{cases} \tag{17}$$

In (16), $i_q^m(k+1)$ and $i_q^p(k+1)$ represent the measured and predicted values of the q-axis current at time $(k+1)T_s$, respectively.

Due to the small difference in the values of network inputs X_{B1} and X_{C1} corresponding to weights B_q and C_{ψ_f}, the target value can be stably reached even if the weights B_q and C_{ψ_f} are not decoupled. However, the values of network inputs X_{A2} and X_{B2} corresponding to weights A_q and B_d are smaller than other network inputs in various forms, so the coupling effects of the two polynomials corresponding to weights A_q and B_d on other terms are quite small, while the coupling effects of other terms on these two polynomials are quite large. Therefore, weights A_q and B_d are not suitable as identification conditions for L_q and L_d. Considering the problem of identification error, this article does not ignore the two polynomials corresponding to weights A_q and B_d. Figure 2 is the control diagram of the proposed method in this article.

4. IMPROVEMENT OF VARIABLE STEP-SIZE FOR ADALINE NEURAL NETWORK PARAMETER IDENTIFICATION METHOD

4.1. Variable Step-Size Design for Traditional Adaline Neural Network Parameter Identification

According to the sigmoid function, the functional relationship between the step-size η and the instantaneous error ε can be constructed. By adjusting the step-size η based on the instantaneous error ε, the internal algorithm can achieve rapid convergence. The sigmoid function prototype is as follows:

$$f(x) = \frac{1}{1+e^{-x}} \tag{18}$$

The traditional variable step-size algorithm adjusts the sigmoid function by simply shifting and flipping it, and adding parameters a, b, and c. Finally, it can obtain a function of the step-size $\eta(k)$ and the absolute value of the instantaneous error $|\varepsilon(k)|$, as shown below:

$$\eta(k) = \frac{1-e^{-a|\varepsilon(k)|^c}}{b+e^{-|\varepsilon(k)|^c}} \tag{19}$$

Parameter a controls the rate of change of the function; parameter b controls the maximum value of the function; and parameter c controls the convergence range of the function.

4.2. Design of Variable Step-Size for Improved Adaline Neural Network Parameter Identification

When there is a parameter mismatch in the motor, the absolute value of the instantaneous error ε and the identification parameter fluctuation will be relatively large during the initial stage of the Adaline neural network parameter identification algorithm. However, after the algorithm has stabilized, there will be a small steady-state error between the instantaneous error ε and the identification parameter. The traditional Adaline neural network parameter identification variable step-size function input is often based on the above range of instantaneous error ε fluctuation and steady-state error range, allowing the step-size η to gradually decrease from a larger step-size or maximum step-size to a smaller step-size or 0 as the instantaneous error ε fluctuates before and after the identification is stable. Since an increase or decrease in the actual parameters of the motor can affect the fluctuation range of the instantaneous error ε, a single variable step-size function with instantaneous error ε as the input will output different step-size ranges for different motor

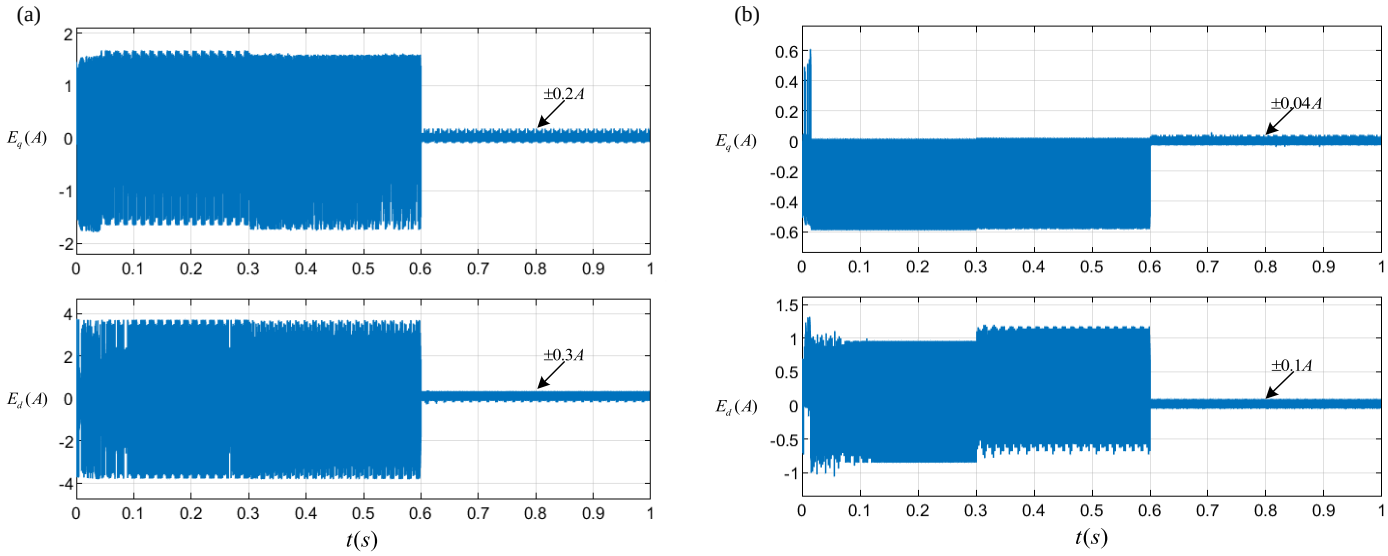

FIGURE 4. Current prediction error of d-axis and q-axis. (a) The motor parameters are 0.5 times the nominal value. (b) The motor parameters are 1.5 times the nominal value.

actual parameters, resulting in inconsistent parameter convergence speed and steady-state fluctuation range.

For the influence of different motor actual parameters on the instantaneous error ε, this paper proposes a variable step-size improvement of the Adaline neural network parameter identification method. This method takes the maximum absolute value of the instantaneous error produced by the maximum step-size input before the identification stabilizes as the classification criterion, and classifies the above maximum absolute value range with different variable step-size functions, where different variable step-size functions represent the actual parameters of the adapted motor. Specifically, at the beginning of identification, a fixed maximum step-size is first input, and based on the current maximum absolute value of the output instantaneous error ε, a variable step-size function corresponding to the classification is selected. Therefore, under different motor actual parameters, the identification waveform can achieve rapid convergence and small steady-state ripple. Figure 3 shows the block diagram of the structure of the wide adaptation variable step-size strategy proposed in this paper.

The following is the variable step-size function proposed in this article.

$$\begin{cases} \eta(k) = \frac{-M_1[1-e^{V(|\varepsilon(k)|-\varepsilon_0)}]}{1+e^{V(|\varepsilon(k)|-\varepsilon_0)}} + M_2 \\ M_1 = \frac{\eta_{\max}-\eta_{\min}}{2} \\ M_2 = \frac{\eta_{\max}+\eta_{\min}}{2} \end{cases} \tag{20}$$

In (20), parameter V controls the rate of change of the function; parameter ε_0 controls the midpoint position of the convergence segment; parameter $\eta_{\max}$ represents the maximum step-size; parameter $\eta_{\min}$ represents the minimum step-size. Compared to traditional variable step-size functions, the variable step-size function proposed in this paper considers the control of the minimum step-size and the midpoint position in the convergence section. When setting parameters, $\eta_{\max}$ and $\eta_{\min}$ can be easily obtained by (10), just based on the instantaneous error ε. Set parameters for the fluctuation range of ε_0, and then adjust the parameter V appropriately. However, when applying traditional variable step-size function, parameters a and c cannot be calculated through any virtual feedback, and continuous adjustment of parameters a and c is necessary. It is obvious that the improved variable step-size function proposed in this article has a more flexible and versatile control of step-size, a wider range of applications, and more convenient parameter settings and adjustments.

5. SIMULATION AND EXPERIMENTAL RESULTS

Due to the difficulty in simulating the parameter variations of physical motors, this article conducts simulation in the MATLAB/Simulink environment and implements hardware in the loop simulation experiments of permanent magnet synchronous motors on the RT-LAB experimental platform. The sampling frequency of simulation and experiment is 10 kHz. The simulation and experiment in this article both adopt the MPCC strategy, and the main parameters of the used motor are shown in Table 1.

TABLE 1. Motor parameters.

Parameter	Description	Value
U_{dc} (V)	DC-bus voltage	310
P_n	Number of pole pairs	4
R_s (Ω)	Stator resistance	0.958
L_d (mH)	D-axis inductance	5.25
L_q (mH)	Q-axis inductance	12
Ψ_f (Wb)	Permanent magnet flux	0.1827
J (kg·m^2)	Moment of Inertia	0.003
B (N·m·s)	Damping coefficient	0.008

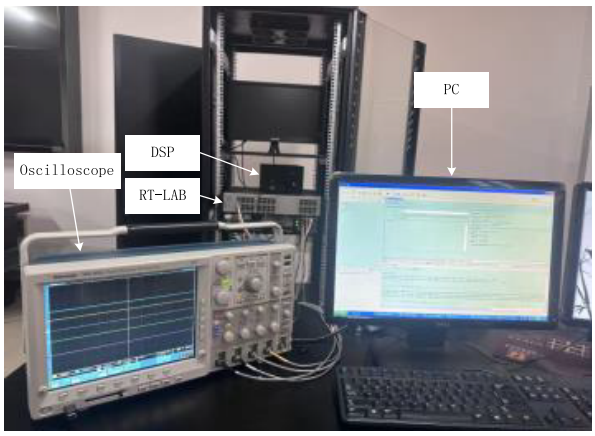

FIGURE 5. RT-LAB experimental platform.

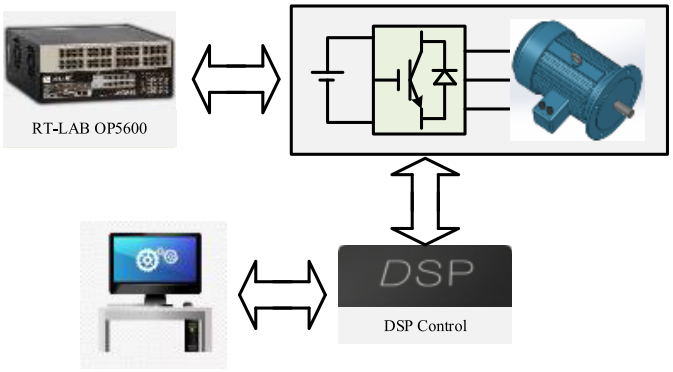

FIGURE 6. RT-LAB hardware in the loop system configuration.

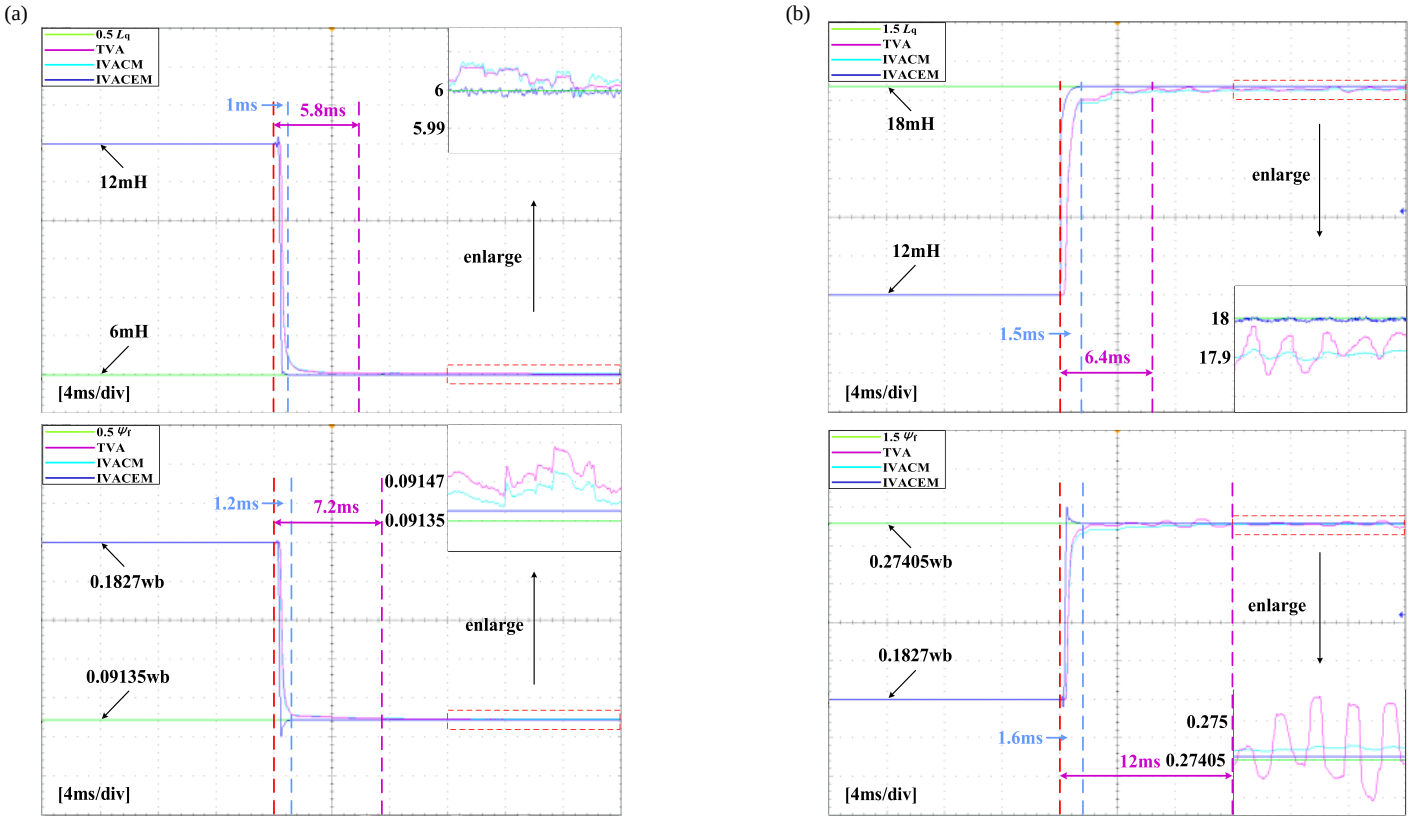

FIGURE 7. Identification results of three identification algorithms for q-axis inductance and permanent magnet flux linkage. (a) The motor parameters are 0.5 times the nominal value. (b) The motor parameters are 1.5 times the nominal value.

The simulation results of the d-axis and q-axis current prediction errors are shown in Figure 4. When the actual motor parameters are 0.5 times and 1.5 times the nominal values, the load torque jump and parameter compensation occur at 0.3 s and 0.6 s, respectively. As can be seen from the figure below, when the motor has a parameter mismatch, regardless of whether the motor is loaded or not, there is a high d-axis and q-axis current prediction error in the system. This has a significant adverse impact on the high-precision control of the system. Therefore, after introducing the identified parameters to the controller at 0.6 s, the d-axis and q-axis current prediction errors significantly decreased, which effectively improved the control accuracy of the system.

The experimental platform consists of a simulation machine OP5600, a DSP controller TMS320F2812, upper computer monitoring equipment, and an oscilloscope in conjunction with relevant software, as shown in Figure 5. The RT-LAB hardware in the loop configuration is shown in Figure 6, and the inverter and PMSM system are constructed using RT-LAB (OP5600).

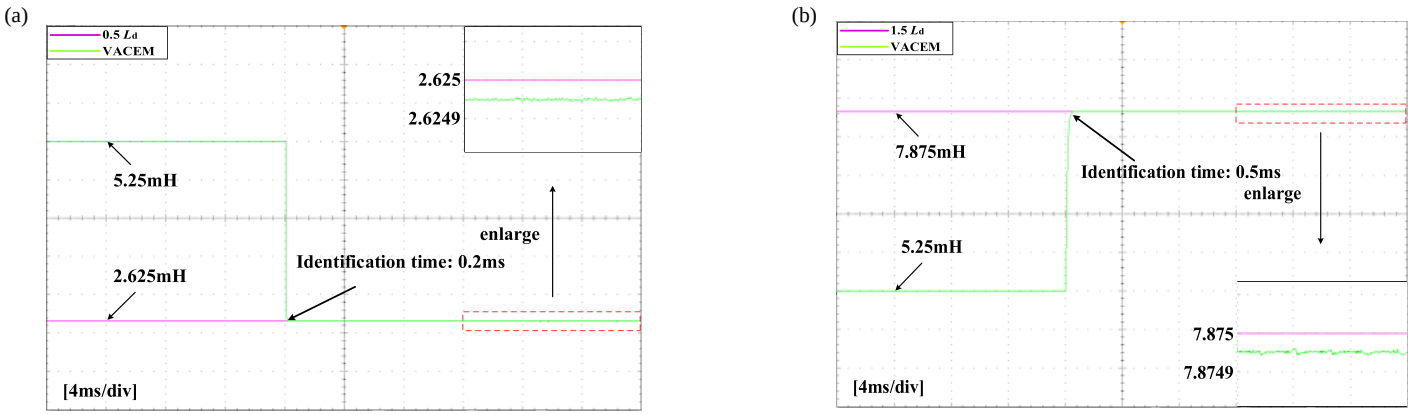

FIGURE 8. Identification results of IVACEM for d-axis inductance. (a) The motor parameters are 0.5 times the nominal value. (b) The motor parameters are 1.5 times the nominal value.

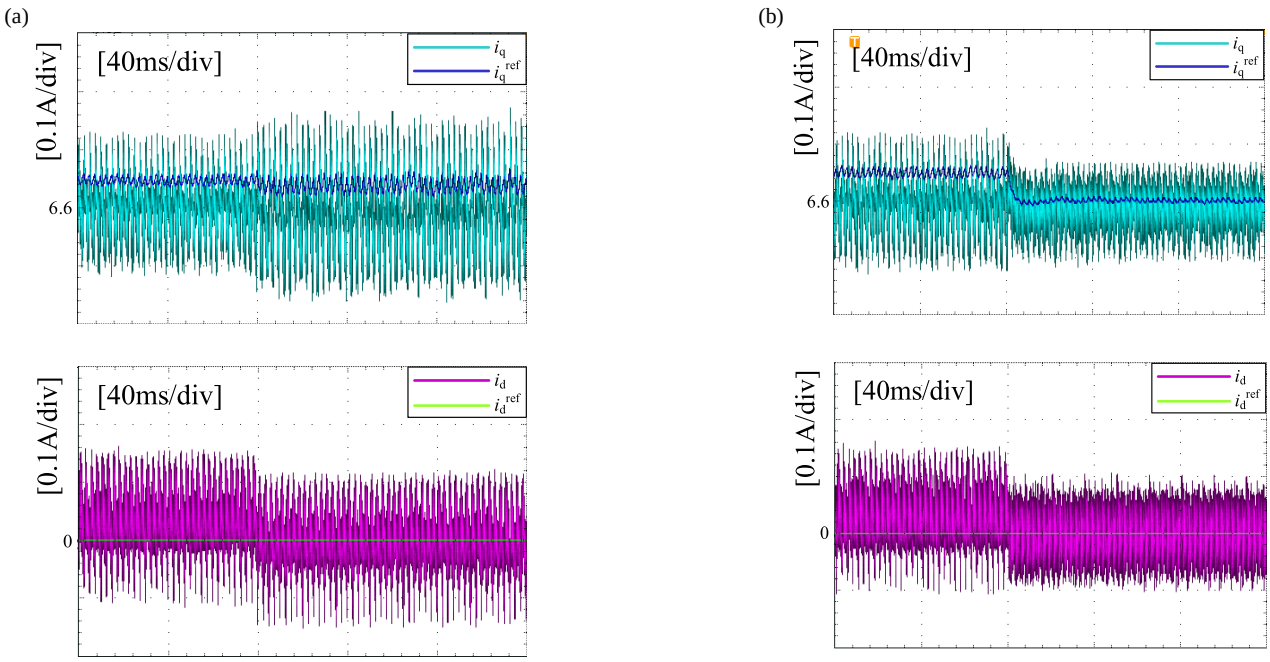

FIGURE 9. d-axis and q-axis current waves before and after parameter compensation. (a) TVA. (b) IVACEM.

When the working speed of IPMSM is 1000 r/min, the load torque is 10 Nm, and the d-axis inductance, q-axis inductance, and permanent magnet flux are both 0.5 times of the nominal value and 1.5 times of the nominal value. The traditional variable step-size Adaline neural network parameter identification algorithm (TVA), the improved variable step-size Adaline neural network parameter identification algorithm based on the traditional model (IVACM), and the improved variable step-size Adaline neural network parameter identification algorithm based on the current prediction error model (IVACEM) are used to identify the current q-axis inductance and permanent magnet flux. The identification results are shown in Figure 7.

Overall, regardless of whether the actual motor parameters are 0.5 times of the nominal value or 1.5 times of the nominal value, the parameter identification time of IVACEM is less than 2 ms. Compared with TVA and IVACM, the identification speed of IVACEM is faster and more stable. After the identification is stable, it can be seen from the comparison of local enlarged images that the q-axis inductance and permanent magnet flux identification stability of IVACEM are better than those of TVA and IVACM. This fully demonstrates that under different motor parameter disturbances, IVACEM has faster identification speed and stronger identification stability than TVA and IVACM.

From a detailed perspective, when the actual parameters of the motor are 0.5 times of the nominal value or 1.5 times of the nominal value, the q-axis inductance and permanent magnet flux identification time of TVA and IVACM remain consistent. This indicates that these two methods have no advantages or disadvantages in identifying speed under different motor parameter disturbances. After the identification is stable, it can be seen from the comparison of local enlarged

images that when the actual parameters of the motor are 0.5 times of the nominal value, the q-axis inductance and permanent magnet flux identification stability of TVA and IVACM are basically the same. When the actual parameters of the motor are 1.5 times of the nominal value, IVACM has better performance in parameter identification stability than TVA. This fully demonstrates that under different motor parameter disturbances, IVACM can maintain identification speed comparable to TVA and has stronger identification stability.

When the working speed of IPMSM is 1000 r/min, the load torque is 10 Nm, and the d-axis inductance is 0.5 times of the nominal value and 1.5 times of the nominal value. The identification results of IVACEM for the current d-axis inductance are shown in Figure 8. This figure reflects the identification ability of IVACEM for d-axis inductance, which has fast identification speed and stable identification results.

When the q-axis inductance, d-axis inductance, and permanent magnet flux are all 1.5 times of the nominal value, the parameters identified by TVA and IVACEM are respectively compensated to the control system at 0.25 seconds. Figure 9 reflects the impact of the above two methods on the dq-axis current when IPMSM operates at a speed of 1000 r/min and a load torque of 10 Nm. After parameter compensation, IVACEM has smaller d-axis and q-axis current ripple, and can basically follow the q-axis current command and d-axis current command. The experimental results indicate that compared to TVA, IVACEM has stronger steady-state performance.

6. CONCLUSION

In order to solve the problem of increased MPCC prediction error caused by IPMSM parameter mismatch, which leads to performance degradation of PMSM control system, this paper proposes an MPC strategy for online parameter identification. The conclusion is as follows:

1) The parameter identification strategy proposed in this article combines the derived and reconstructed current prediction error model with the Adaline neural network parameter identification algorithm. By identifying the mismatch multiple of the motor parameters, the motor parameters themselves are identified. Compared to the traditional Adaline neural network parameter identification algorithm, the strategy proposed in this paper can be applied to IPMSM, with faster identification speed and higher identification accuracy.

2) The paper proposes a variable step-size algorithm that adapts the absolute value of the instantaneous error for different ranges to the variable step-size function with different actual parameters of the motor. This enables different actual motor parameters to correspond to different variable step-size functions, resulting in more stable identification accuracy. This greatly improves the algorithm's adaptability to different motor parameter disturbance ranges. In addition, a novel variable step-size function is proposed, which has simpler parameter tuning and easier debugging than traditional variable step-size functions. Finally, it has been demonstrated through experiments that compared to the traditional variable step-size Adaline neural network parameter identification algorithm, the parameter identification algorithm described in this paper has significant advantages in real-time compensation of multiple parameters.

ACKNOWLEDGEMENT

This work was supported by the Scientific Research Fund of Hunan Provincial Education Department under Grant Number 23B1017, Natural Science Foundation of Hunan Province of China under Grant Number 2022JJ50094.

REFERENCES

[1] Xu, Y., S. Li, and J. Zou, "Integral sliding mode control based deadbeat predictive current control for PMSM drives with disturbance rejection," *IEEE Transactions on Power Electronics*, Vol. 37, No. 3, 2845–2856, Mar. 2022.

[2] Li, S., M. Zhou, and X. Yu, "Design and implementation of terminal sliding mode control method for PMSM speed regulation system," *IEEE Transactions on Industrial Informatics*, Vol. 9, No. 4, 1879–1891, Nov. 2013.

[3] Repecho, V., D. Biel, and A. Arias, "Fixed switching period discrete-time sliding mode current control of a PMSM," *IEEE Transactions on Industrial Electronics*, Vol. 65, No. 3, 2039–2048, Mar. 2018.

[4] Li, S. and H. Gu, "Fuzzy adaptive internal model control schemes for PMSM speed-regulation system," *IEEE Transactions on Industrial Informatics*, Vol. 8, No. 4, 767–779, Nov. 2012.

[5] Yuan, X., S. Zhang, and C. Zhang, "Improved model predictive current control for SPMSM drives with parameter mismatch," *IEEE Transactions on Industrial Electronics*, Vol. 67, No. 2, 852–862, Feb. 2020.

[6] Abu-Rub, H., J. Holtz, J. Rodriguez, and B. Ge, "Medium-voltage multilevel converters — State of the art, challenges, and requirements in industrial applications," *IEEE Transactions on Industrial Electronics*, Vol. 57, No. 8, 2581–2596, Aug. 2010.

[7] Fang, Y. and Y. Xing, "Design and analysis of three-phase reversible high-power-factor correction based on predictive current controller," *IEEE Transactions on Industrial Electronics*, Vol. 55, No. 12, 4391–4397, Dec. 2008.

[8] Mohamed, Y. A.-R. I. and E. F. El-Saadany, "A control scheme for PWM voltage-source distributed-generation inverters for fast load-voltage regulation and effective mitigation of unbalanced voltage disturbances," *IEEE Transactions on Industrial Electronics*, Vol. 55, No. 5, 2072–2084, May 2008.

[9] Kakosimos, P. and H. Abu-Rub, "Deadbeat predictive control for PMSM drives with 3-L NPC inverter accounting for saturation effects," *IEEE Journal of Emerging and Selected Topics in Power Electronics*, Vol. 6, No. 4, 1671–1680, Dec. 2018.

[10] Zeng, Q. and L. Chang, "An advanced SVPWM-based predictive current controller for three-phase inverters in distributed generation systems," *IEEE Transactions on Industrial Electronics*, Vol. 55, No. 3, 1235–1246, Mar. 2008.

[11] Zhang, Z., Y. Liu, X. Liang, H. Guo, and X. Zhuang, "Robust model predictive current control of PMSM based on nonlinear extended state observer," *IEEE Journal of Emerging and Selected Topics in Power Electronics*, Vol. 11, No. 1, 862–873, Feb. 2023.

[12] Yang, M., X. Lang, J. Long, and D. Xu, "Flux immunity robust predictive current control with incremental model and extended state observer for PMSM drive," *IEEE Transactions on Power Electronics*, Vol. 32, No. 12, 9267–9279, Dec. 2017.

[13] Lin, C.-K., T.-H. Liu, J.-T. Yu, L.-C. Fu, and C.-F. Hsiao, "Model-free predictive current control for interior permanent-magnet synchronous motor drives based on current difference detection technique," *IEEE Transactions on Industrial Electronics*, Vol. 61, No. 2, 667–681, Feb. 2014.

[14] Yao, Y., Y. Huang, F. Peng, J. Dong, and H. Zhang, "An improved deadbeat predictive current control with online parameter identification for surface-mounted PMSMs," *IEEE Transactions on Industrial Electronics*, Vol. 67, No. 12, 10 145–10 155, Dec. 2020.

[15] Boileau, T., N. Leboeuf, B. Nahid-Mobarakeh, and F. Meibody-Tabar, "Online identification of PMSM parameters: Parameter identifiability and estimator comparative study," *IEEE Transactions on Industry Applications*, Vol. 47, No. 4, 1944–1957, Jul.-Aug. 2011.

[16] Bui, M. X., M. F. Rahman, D. Guan, and D. Xiao, "A new and fast method for on-line estimation of d and q axes inductances of interior permanent magnet synchronous machines using measurements of current derivatives and inverter DC-bus voltage," *IEEE Transactions on Industrial Electronics*, Vol. 66, No. 10, 7488–7497, Oct. 2019.

[17] Yang, Z. J. and L. N. Wang, "Online multi-parameter identification for surface-mounted permanent magnet synchronous motors," *Transactions of China Electrotechnical Society*, Vol. 29, No. 3, 111–118, Mar. 2014.

[18] Liu, J. H. and W. Chen, "Online multi-parameter identification for surface-mounted permanent magnet synchronous motors under quasi-steady-state," *Transactions of China Electrotechnical Society*, Vol. 31, No. 17, 154–160, Sep. 2016.

[19] Kumar, R., R. A. Gupta, and A. K. Bansal, "Identification and control of PMSM using artificial neural network," in *2007 IEEE International Symposium on Industrial Electronics*, 30–35, Vigo, Spain, 2007.

[20] Liu, K. and J. Zhang, "Adaline neural network based online parameter estimation for surface-mounted permanent magnet synchronous machines," *Proceedings of the CSEE*, Vol. 30, No. 30, 68–73, Oct. 2010.

[21] Zhang, L. W., P. Zhang, Y. F. Liu, C. Zhang, and J. Liu, "Parameter identification of permanent magnet synchronous motor based on variable step-size adaline neural network," *Transactions of China Electrotechnical Society*, Vol. 33, No. S2, 377–384, Dec. 2018.

[22] Wang, Z., M. Yang, L. Gao, Z. Wang, G. Zhang, H. Wang, and X. Gu, "Deadbeat predictive current control of permanent magnet synchronous motor based on variable step-size adaline neural network parameter identification," *IET Electric Power Applications*, Vol. 14, No. 11, 2007–2015, Nov. 2020.

[23] Zhang, X., L. Zhang, and Y. Zhang, "Model predictive current control for PMSM drives with parameter robustness improvement," *IEEE Transactions on Power Electronics*, Vol. 34, No. 2, 1645–1657, Feb. 2019.